

Soft Matter

Accepted Manuscript



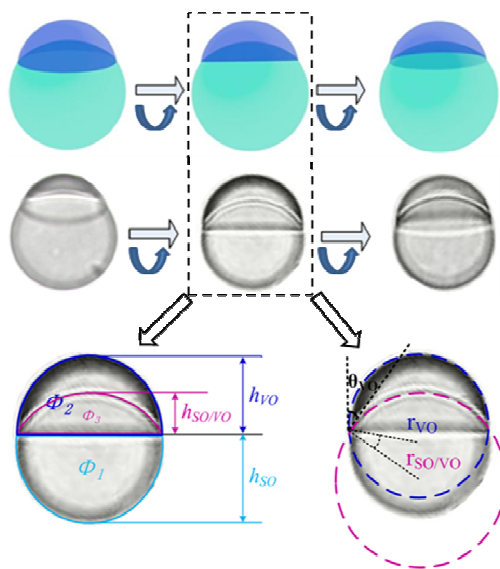
This is an *Accepted Manuscript*, which has been through the Royal Society of Chemistry peer review process and has been accepted for publication.

Accepted Manuscripts are published online shortly after acceptance, before technical editing, formatting and proof reading. Using this free service, authors can make their results available to the community, in citable form, before we publish the edited article. We will replace this *Accepted Manuscript* with the edited and formatted *Advance Article* as soon as it is available.

You can find more information about *Accepted Manuscripts* in the [Information for Authors](#).

Please note that technical editing may introduce minor changes to the text and/or graphics, which may alter content. The journal's standard [Terms & Conditions](#) and the [Ethical guidelines](#) still apply. In no event shall the Royal Society of Chemistry be held responsible for any errors or omissions in this *Accepted Manuscript* or any consequences arising from the use of any information it contains.

Graphical abstract



Projection of rotationally and translational free droplets of Janus emulsions between slides with spacers and the topology elements of Janus droplets

Droplet Topology Control of Janus Emulsion Prepared in One-Step High Energy Mixing

*Lingling Ge, Wanqing Shao, Shuhui Lu, Rong Guo**

School of Chemistry and Chemical Engineering, Yangzhou University, Jiangsu Province 225002 People's

Republic of China

*To whom correspondence should be addressed. E-mail: guorong@yzu.edu.cn. Fax: (+86)-514-87311374.

Abstract: Droplet topology of Janus emulsion in the system of vegetable oil (VO)/silicone oil (SO)/Tween 80 aqueous solution (Aq) prepared in one-step high energy mixing is investigated mainly by image observation. Quantitative information is analyzed of the topology referring to the curvature of VO/SO interface, the location of contact plane, and the volume ratio of VO/SO within individual droplets. The results show that the “stable Janus emulsion” region in the phase map enlarges with the surfactant concentration. The average volume ratio of two oil lobes within individual Janus droplet agrees with the emulsion composition in the “stable Janus emulsion” region, which means that the droplet topology can be controlled by the emulsion preparation process within realistic limits. The volume ratio of VO/SO within individual droplet ranges from about 0.54 to 0.17 in the system of VO/SO/3 wt% Tween 80_(aq), beyond which separate VO and SO droplets are observed. The topology of Janus droplet is found to be determined by both the contact angle of three liquids in the contact line and the location of the contact plane. The contact angle of oil cap is determined by the interfacial tension referring to the local equilibrium. The location of the contact plane is the dominant factor determining the volume ratio of two oil lobes. Composition change of emulsion results in the corresponding tune of the location of contact plane and subsequently, the volume ratio of two oils within Janus droplets.

1 Introduction

One of the most essential research areas in colloid chemistry is the properties of emulsions,¹⁻³ covering the entire range from their formation⁴ to the question of their colloidal stability.⁵ In addition to the simple emulsions, the multiple emulsions⁶ have attracted attention from the initial period of preparation through consecutive stages⁷⁻¹¹ to subsequent one-step processes.¹² These contributions were mainly empirical attempts to find successful bulk preparation methods to formulations with satisfactory stability. The research approach went through a metamorphose with the application of micro fluidic processes.^{13, 14} The process made possible the preparation of different complex emulsions^{15, 16} and a large number of applications.¹⁷

The micro fluidic preparation of Janus droplets takes place with one droplet at a time from a capillary; energetically at the lowest level, in contrast to the traditional preparation by different kinds of mixing.⁴ Hence, drops are close to local equilibrium and a correlation is strongly expected for between drop morphology and interfacial tension equilibrium at the three-liquid contact line. This connection was confirmed by an elegant recording¹⁸ of the equilibration process from a totally engulfed drop of tetradecane/tripropylene glycol diacrylate in a 1 % aqueous solution of sodium dodecylsulfate to a Janus drop; a process lasting 1 second, of which the diffusion of the engulfed drop to the interface took most of the time. The correlation between topology and interfacial tensions subsequently was comprehensibly tested in micro fluidic experiments by Guowski et. al¹⁷ giving topologies in excellent agreement with predictions from calculations based on interfacial tensions. All these evaluations were based on the extremely low energy involved in the micro fluidic process, and a local equilibrium would be expected.

Surprisingly, the even more complex Janus emulsions in a one-step high energy mixing process recently introduced,¹⁹⁻²¹ indicated a correlation between droplet topology and interfacial tension equilibrium. Nevertheless, the experimental droplet topologies indicated the interfacial tensions at the contact line have

a significant guidance on the final topology, in spite of the high energy input, including a final shear between the microscope slide and the cover glass. However, the limited experimental investigations of these emulsions,¹⁹⁻²¹ especially for Janus emulsions of high complexity, indicate a definite need for additional determinations of the topology of such systems.

2 Experimental

2.1 Materials

Silicone oil (SO, DC Fluid 50 CST) was obtained from Dow Corning, the density of SO was 0.962 g/cm^3 ; vegetable oil (VO, Sunflower oil) was obtained from Grain Food Marketing Co., Ltd and used as received, the density of VO was 0.920 g/cm^3 ; surfactant (Tween 80, 97 wt%) was purchased from Aladdin Reagent Co., Ltd; deionized water.

2.2 Emulsion preparation

A series of samples with different weight fractions of silicone oil (SO), vegetable oil (VO), and aqueous solution of Tween 80 (Aq) were weighed into 10 mL test tubes. The compositions of the initial emulsions were given in Table1, which outlined the three series with Aq occupying weight fractions 0.10, 0.20 and 0.30, designated as series 1, 2 and 3. Within each series, the volume ratios of VO/SO were approximately 0.50, X; 0.25, Y; and 0.17, Z. The samples were mixed using the vortex mixer (Kylin-Bell Lab Instruments Co.,Ltd) at the speed of 3000 rpm for 2 min. Photographs of emulsions in tubes were taken with digital camera with six mega pixels (Canon IXUS 65).

2.3 Determination of partial phase map

The stable emulsion region was determined by the transition point from phase separation within 24 h to no phase changes after 24 h by adding Aq to the samples with different weight ratios of VO/SO. The

transition points were checked by adding SO into the samples with different weight ratios of VO/Aq. All the samples were placed in a thermostat at 25 ± 0.1 °C.

2.4 Microscope

The emulsions for microscope experiment were diluted with Aq, each being weight ratio of emulsion: Aq=2:1. The test tube was turned up and down very gently to homogenize the mixture without disturbing the existing emulsion droplets.²² A small amount of diluted emulsion was placed on a pre-cleaned 76×25 mm microscopic slide (Guanghui health-care Factory) and then gently covered with a 17×17 mm micro cover glass (Jinglun Glass Industries, Inc.). Copper wires with diameter of 90 μm were used as spacers to ensure free rotation of all emulsion droplets. All pictures were taken by microscope from Germany Leica Instrument Co., Ltd with a magnification of ×20. More than fifty droplets of each sample were analyzed to get the average topology parameters. The error of volume ratio was within ± 0.18 , and error of contact angle was within $\pm 2.3^\circ$.

2.5 Interfacial tension measurement

Interfacial tensions were measured by the pendant drop method using an interface tension meter (Dataphysic Instrument Co., Ltd, Germany). A droplet was attached at the end of a stainless nozzle (outer diameter of 1.65 mm) connected to a syringe. A backlight source and a camera with microscopic zoom lens were used to capture the images of the droplets. The metallic nozzle was washed with ethanol and deionized water with sonication, and then dried in air before use. The interfacial tension value was recorded 10 min after the droplet was pumped into the liquid to ensure the equilibrium. All measurements were repeated more than 8 times and in each measurement, an old droplet was dispensed and a new pendant drop was measured.

2.6 Size distribution measurement

The diameter distribution of the emulsion droplets was determined by a BT-9300H laser particle size analyzer (Bettersize Instruments Ltd., China). The emulsion was slowly added into water with gentle stirring at speed of 320 rpm, and the diluted sample was then pumped into the detector at 1500 mL/min. Each measurement lasted 1 min, and the measurements were repeated more than 3 times. All experiments were conducted at 25 ± 0.1 °C.

3 Results

3.1 Composition of Stable Janus Emulsion

The photographs of three series, Table 1, of emulsions offer information about the change in stability as well as about the destabilization action, Figure 1. The aqueous mass fraction A_q is equal to 0.10 in the first series, 0.20 in series 2, and 0.30 in series 3. The VO/SO mass ratio decreases from 0.50 to 0.25 to 0.17 from left to right in each series. The photographs are taken at 24 h after the emulsification when the development of each layer reaches stable state, and no further change is observed even after six months (Figure S1). Obvious phase separation occurs in series 1 with series of layers from the top; VO, SO, emulsion, and a small aqueous layer. The final volumes of each layer separated are shown in Table S1. The volume of VO layer separated in series 1 decreases from 1.82 mL of X1 to 0.74 mL of Z1, and the separated SO layer increases from 2.42 mL of X1 to 3.68 mL of Z1, which is in accordance to the initial composition in Table 1. The complex destabilization mechanism of emulsions has been reported¹⁹ and is considered outside the present contribution. No obvious phase separation is observed in series 2, which indicates the stability of emulsion, while an aqueous phase is separated at the bottom of series 3. Final composition of stable emulsions in the three series can be obtained from the initial and final volumes. As shown in Table 2, the volume ratios VO/SO of all the three stable emulsions in series 1 remain constant at a lower value of about 0.11-0.16, which is independent on the initial sample

composition, 0.57 to 0.17 in Table 1. While the volume ratios of VO/SO in the stable emulsions of series 2 decrease from 0.55 of X2 to about 0.15 of Z2, which is in agreement with the initial volume ratio. The VO/SO numbers in series 3 are the same with the corresponding ones in series 2. As for the weight fractions of Aq in the final stable emulsion, the values in series 1 are approximately 0.22-0.29, which are higher than the initial composition, 0.10 in Table 1, due to the phase separation of VO and SO. The weight fractions of Aq in series 2 are the same with initial composition, 0.20, which is a reasonable outcome since all the initial components are emulsified. As for the case in series 3, weight fractions of Aq are the same with series 2 at 0.20, though the initial value is 0.30 indicating that the extra Aq in series 3 is separated out.

“Stable Janus emulsion” is defined in the present contribution for the case of no phase separation prepared for 24 h as the case in series 2. The composition limits for stable emulsions are given in Figure 2, revealing a gradual enlargement of the region with rising content of surfactant in the Aq. The maximum and minimum weight fractions of Aq in the emulsion as shown in Table S2 increase from the range of 0.26-0.18 at Tween 80 content of 1 wt% to 0.33-0.10 at 5 wt%, while the range of VO/SO is enlarged from 0.41-0.27 for 1 wt% Tween 80_(aq) to 0.69-0.06 for 5 wt% Tween 80_(aq).

3.2 Topology of Janus Emulsion Droplets

A typical emulsion sample, Y2, is used to investigate the topology uniformity of emulsion droplets against the height of emulsion layer. No obvious difference of topology is observed comparing the microscope images of samples taken from top, middle, and bottom of emulsion layers (Figure 3). All images are populated entirely by regular Janus droplets, and each droplet is composed of lobes of two oils against the background of aqueous solution. The darker “caps” of the droplet is VO, while the other lobe is SO.²¹ Size distributions of emulsion droplets from different heights of the emulsion layers show a uniform size distribution (Figure 4); an additional indication of the stability of emulsion.

Investigation on the effect of the oil volume ratios on the droplet topology is limited to samples from the middle of the emulsion layer, since the photographs in Figure 3 and 4 show the drop size and topology to be invariant with height of the emulsion layer. The result in Figure 5 shows that all the micrographs are populated with Janus topology. For the emulsions in series 1, the images of VO caps are relatively small, and no obvious difference is observed comparing all the three micrographs. As a contrast, the three emulsions in series 2 show an apparent difference with the VO/SO volume ratio. Image from emulsion X2 with highest volume ratio of VO/SO is populated with Janus droplets with obviously larger VO caps, while the volume of VO cap diminishes with reducing VO/SO ratio, from X2 to Z2. The relevance of optical microscopy image with the topology of Janus droplets in bulk emulsions is of vital importance in the present investigation. Relevant research has been performed by Friberg's group,²² indicating the microscope images to provide realistic information about the droplet topology of the emulsion in bulk, in spite of the specific effect of the shear on the sample between the cover glass and the planar slide; as well as of the wetting effect of the glass surfaces on the emulsion droplets. Based on these earlier results, the representations in Figure 5 provide a central conclusion i. e. the topology of Janus droplets can be tuned by the composition of the stable emulsions. A quantitative relationship between the volume ratio of two oils within individual Janus droplets and the total emulsion composition is presented in the Discussion section. As for the images of emulsions in series 3, the configurations in the three micrographs are the same with the corresponding ones in series 2. The result is expected, because extra aqueous phases in series 3 are separated out from emulsion and subsequently, the final compositions of emulsion are the same with emulsions in series 2. Size distributions of emulsion droplets in the three series show no obvious difference between the emulsions with mean diameter of about 60 μm (Figure 6).

3.3 Interfacial Tensions

The interfacial tensions between the aqueous phase and the oils are given in Table 3. The numbers are at a realistic level^{23, 24} and show a modest decrease with increased concentration in the aqueous phase; which is a rational outcome, since the concentrations are significantly greater than the critical micellization concentration of the specific surfactant.²⁵

The basics of the relationship between the interfacial tensions and contact angles of Janus droplets, Figure 7A, have been recently reported and the angles α , β , and δ are directly obtained from interfacial tension values in Table 3:^{17, 26-28}

$$\cos \alpha = 1/2 \left(\gamma_{W/VO}^2 + \gamma_{VO/SO}^2 - \gamma_{W/SO}^2 \right) / \gamma_{W/VO} \gamma_{VO/SO} \quad (1)$$

$$\cos \beta = 1/2 \left(\gamma_{W/VO}^2 + \gamma_{W/SO}^2 - \gamma_{VO/SO}^2 \right) / \gamma_{W/VO} \gamma_{W/SO} \quad (2)$$

$$\cos \delta = 1/2 \left(\gamma_{W/SO}^2 + \gamma_{VO/SO}^2 - \gamma_{W/VO}^2 \right) / \gamma_{W/SO} \gamma_{VO/SO} \quad (3)$$

Within VO caps the angle θ_{VO} equals to $\beta + \delta$. The calculated θ_{VO} values in Table 3 show obvious enlargement from 27° to 40° with increasing weight fraction of Tween 80 in Aq from 0.1 wt% to 9 wt%, notwithstanding the interfacial tensions between random two liquids are relatively constant; illustrating the range of emulsion topology centered on the one expected from the interfacial tension equilibrium.

4 Discussion

4.1 Local equilibrium at the contact line of Janus droplets

The results add to the understanding of two factors in the high energy emulsification to form Janus emulsion; the relative volume ratio of the two oils and the local equilibrium at the contact line between the three liquids. Janus emulsions prepared by micro fluidic with the ultimately gentle emulsification present excellent agreement between the expected topology for droplets of local equilibrium and experimental

results.¹⁷ However, there is no justification to assume that equilibrium conditions are prevalent during the ongoing emulsification process for the Janus emulsions formed in a one-step high energy process. Hence, the Janus topology is anticipated to appear first after the moment of ceased agitation, when the energy level of the system is reduced. Hence, the topology is a result of a kinetic process and the fraction of separated mono-oil and Janus droplets may conceivably be estimated only by a Boltzmann distribution from the free energy difference. In addition, the formation of droplets with extreme coverage of one oil by the other may not be kinetically favored although the local equilibrium allows for a wide range of volume ratios between the two oils. In the following narrative these two factors will be examined, beginning with the importance of local equilibrium.

The basis for the examination is the difference in surface free energy for the two cases; in which the two oils form separate droplets and Janus droplets; assuming local equilibrium at the contact angle.¹⁷ The cross-section of the Janus droplets is presented in Figure 7 with the definition of r and h in eq. 4 illustrated. The radiuses of two hemispheres are assumed to be the same and the average value of $r=30\ \mu\text{m}$ is taken according to the size distribution curve as well as microscopy images. Accordingly, the average radius R of the VO/SO interface is about $35\ \mu\text{m}$ according to the results of microscopy images. Three values for interfacial tensions $\gamma_{\text{VO/SO}}=2.54\ \text{mN/m}$, $\gamma_{\text{VO/Aq}}=7.22\ \text{mN/m}$, $\gamma_{\text{SO/Aq}}=9.39\ \text{mN/m}$, Table 3, are used for calculation. Assuming a realistic number $h=r/2$ according to results from microscopy images, the volumes V_{cap} and the area A_{cap} of VO and SO as sphere caps are calculated using standard integration:

$$V_{\text{cap}} = \pi h^2 (3r - h)/3 \quad (4)$$

$$A_{\text{cap}} = 2\pi r h \quad (5)$$

The essential numbers are presented in Table 4. Comparing with the results of separate droplets, the interface area of Janus is higher mainly contributed by the interface of two oils. However, the Janus

droplet has a total interface free energy of $1.08\text{E-}10$ J which is less than the two separate droplets $1.19\text{E-}10$ J. Thus, a Boltzmann distribution overwhelmingly favors the Janus structure and it appears that this topology is heavily preferred as a final local equilibrium state.

4.2 Topology of Janus droplets

5 Two essential features determining the equilibrium topology of a Janus droplet (O1+O2)/W with fixed size are the curvature of VO/SO interface and the location of contact plane. The curvature is characterized by the contact angle of δ , which is determined by the interfacial tension equilibrium at the contact line between the three liquids. The location of contact plane is also a consequence of the droplet composition, which is related to the relative amount of two oils in emulsion preparation. The combined effect of these
10 two independent elements results in various values of the volume ratios of the two oils.

In the following discussion, the geometrical parameters of contact angle θ_{VO} , the location of contact plane τ_{cp} , and the volume ratio VO/SO are extracted from the microscopy images. This evaluation critically depends on choosing droplets with a specific orientation and that the interaction with the glass surfaces is negligible.^{22, 29} Copper wires with diameter of droplet size are used as spacers between slides and cover
15 glass to avoid the distortion of the droplets in the present experiments. Examples of configurations on the photograph of Figure 8A verify the free rotation of all droplets. Five typical textures from the photograph are taken and ascribed to five rotating modes as illustrated in Figure 8A. The projection of VO/SO interface profile and that of the three phase contact lines result in three curves in the image within each droplet. The sharp dark curve is the projection of the interface between VO and SO. The white curve and
20 the vague dark curve come from the projection of the contact line of the three phases. Correct values of the contact angles are obtained from the case with the projection of three phase contact line overlapping and appearing as a straight line, middle projection of Figure 8A, as demonstrated in Figure 8B.

The angle can be obtained by the angle of two radius lines crossing on the three phase contact line as shown in Figure 8B. It should be noted that the partial interfaces are assumed as part of a sphere and the effect of distortions from the colloidal stability of thin films is neglected.³⁰⁻³² In addition, the parameter of τ_{cp} is employed to characterize the location of contact plane and defined as follows:

$$\tau_{cp} = \frac{h_{VO}}{h_{VO} + h_{SO}} \quad (6)$$

Where h_{SO} , h_{VO} , and $h_{SO/VO}$ are correspond to the heights of three caps as shown in Figure 8C. The straight line is the projection of the contact line, and standard integrals are used to obtain the volumes Φ_1 to Φ_3 which represent the volume of three caps based on the plane of the three phase contact circle and on the interfaces of SO/Aq, VO/Aq, and VO/SO, respectively. The volumes of VO and SO are subsequently obtained by pair wise combinations of Φ_1 to Φ_3 as shown in equation 7:

$$VO/SO = \frac{\phi_2 - \phi_3}{\phi_1 + \phi_3} = \frac{\pi h_{VO}^2 (r_{VO} - h_{VO}/3) - \pi h_{SO}^2 (r_{SO} - h_{SO}/3)}{\pi h_{SO}^2 (r_{SO} - h_{SO}/3) + \pi h_{SO}^2 (r_{SO} - h_{SO}/3)} \quad (7)$$

Where r_{VO} , r_{SO} , and $r_{SO/VO}$ are the fitted radii from the partial circles of VO, SO phases, and the VO/SO interface.

Table 2 shows the geometrical details of Janus droplet from microscopy image. All the average contact angles of VO caps obtained are within 34°-38°, which are considered to be constant irrespective to the initial composition within the statistical error. This is reasonable because the surfactant concentration in the aqueous phase is kept constant at 3 wt%, and we can safely deduce that the interfacial concentrations of surfactant in the systems investigated are the same because only the relative amount of oil phases are changed. Hence, the same interfacial tensions of all the samples in the three series result in the constant contact angle. In addition, the value obtained from microscopy image agrees with the value calculated

from the interfacial tension, 36° . The agreement between the topology calculated from local equilibrium and the experimental results from micro fluids is rational because distinctly minimum energy is input in preparation of Janus droplets. Recent reports by Friberg et al.^{22, 27, 33} pointed out a connection between the kinetically formed emulsions and local equilibrium topology of Janus droplets prepared from one-step high energy mixing, similar to the results from micro fluid emulsion. In the present contribution, the agreement of experimental results with interfacial tension also suggests that the droplets between slides are close to local equilibrium. The location of contact plane τ_{cp} shows pronounced dependence on the composition of emulsion. As shown in Table 2, all the τ_{cp} values of emulsions in series 1 remain constant at a lower value of approximately 0.44, which is expected since the final compositions of emulsions in this series are the same. The τ_{cp} values in series 2 and 3 show obvious decrease from a relative higher number of about 0.47 to 0.44 with reduced VO fraction.

The trend of the volume ratio change of VO/SO within individual droplets agrees well with τ_{cp} for all nine samples, suggesting that the relative volume is determined by the location of the contact plane; as expected for a local equilibrium system with constant contact angle. What is more essential, the volume ratio of the two oils within individual droplets is of the same magnitude as the ratio of VO/SO in the stable emulsion composition as shown in Table 2. This agreement indicates that the droplet topology can be tuned by initial composition of emulsion during the preparation process, provided the emulsion is within the region of stable emulsions in Figure 2. The volume ratio of VO/SO of Janus droplet can be tuned from 0.54 to 0.17 in the system of VO/SO/3 wt% Tween 80_(aq).

The emulsion composition referring to the three liquids is kept constant at VO/SO=0.25 and weight fraction at Aq=0.20. The content of surfactant in the liquids of Aq is changed in order to inspect the effect of interfacial tension on the topology of Janus droplets. Statistic results from microscope images in Table 3 show that the contact angle of VO cap increases with the content of Tween 80, from about 30° for 0.1

wt% Tween 80 to 39° for 9 wt% Tween 80, which is in agreement with the calculated value from interfacial tension. However, the average volume ratio of VO/SO within individual droplets is kept constant at about 0.28 irrespective the obvious increase of contact angle. As for the location of contact plane, the τ_{cp} value as shown in Table 3 keeps constant at 0.46. The results indicate that the location of contact plane is the decisive factor of the volume ratio of two oil hemispheres within Janus droplets.

Conclusions

Microscopy photograph of rotationally and translational free droplets of Janus emulsion (O1+O2)/Aq between slides with spacers is used to get quantitative topology parameters including the contact angle, the location of the contact plane, and the volume ratio of two oils within Janus droplets. The “stable Janus emulsion” region in the phase map of VO/SO/Tween 80_(aq) is of vital to the present investigation, because the control of droplet topology by emulsion composition can only be realized within this region. The region is enlarged with the content of Tween 80 in the aqueous phase. More essentially, the volume ratio of two oil lobes within Janus droplets agrees with the emulsion composition within the stable emulsion region. Hence, the droplet topology can be controlled by initial composition of emulsion. The average volume ratio of VO/SO of Janus droplets in the system of VO/SO/3 wt% Tween 80_(aq) varies from about 0.54 to 0.17, which can be tuned by the composition of emulsion.

The topology of Janus droplets is determined by both the contact angle of three liquids in the contact line and the location of the contact plane. The contact angle of oil cap is determined by the interfacial tension referring to the local equilibrium. Surfactant concentration change in aqueous solution realizes the adjustment of the topology. The location of the contact plane is the dominant factor determining the volume ratio of two oils. Composition change of emulsion causes the corresponding adjustment of the location of contact plane and subsequently, the volume ratio of two oils within Janus droplets.

Acknowledgements

The authors are grateful to Prof. Stig. E. Friberg for his valuable help. This work was financially supported by the National Nature Science Foundation of China (No. 21203162, 21073156), Project Funded by the Priority Academic Program Development of Jiangsu Higher Education Institutions, and Natural Science Fund for Colleges and Universities in Jiangsu Province (No. 13KJ13150040).

References

1. B. P. Binks, *Modern Aspects of Emulsion Science*, Cambridge, UK, 1998.
2. J. Sjoblom, *Encyclopedic Handbook of Emulsion Technology*, Marcel Dekker, N.Y., 2001.
3. F. Leal-Calderon, J. Bibette and V. Schmitt, *Emulsion Science: Basic Principles*, N. Y., 2007.
4. S. E. Friberg, "Emulsion Formation" in *Encyclop*, Colloid Interface Sci. T., (in press).
5. J. Sjoblom, *Emulsion and Emulsion Stability, 2nd Ed.*, CRC Press LLC, Boca Raton, FL, 2006.
6. A. Aserin, *Multiple Emulsions: Technology and Applications*, New Jersey, 2008.
7. S. Matsumoto, Y. Kita and D. Yonezawa, *Journal of Colloid and Interface Science*, 1976, **57**, 353-361.
8. V. B. Menon and D. T. Wasan, *Separation Science and Technology*, 1988, **23**, 2131-2142.
9. N. Garti, *Colloids and Surfaces A: Physicochemical and Engineering Aspects*, 1997, **123–124**, 233-246.
10. R. Aveyard, B. P. Binks and J. H. Clint, *Advances in Colloid and Interface Science*, 2003, **100–102**, 503-546.
11. J. A. Hanson, C. B. Chang, S. M. Graves, Z. Li and T. G. Mason, *Nature*, 2008, **455**, 85-88.
12. J. M. Morais, O. D. H. Santos, J. R. L. Nunes, C. F. Zanatta and P. A. Rocha-Filho, *Journal of Dispersion Science and Technology*, 2008, **29**, 63-69.
13. M. Joanicot and A. Ajdari, *Science*, 2005, **309**, 887-888.
14. T. Nisisako, S. Okushima and T. Torii, *Soft Matter*, 2005, **1**, 23-27.
15. M. Hashimoto, P. Garstecki and G. M. Whitesides, *Small*, 2010, **3**, 1792-1802.
16. H. C. Shum, A. R. Abate, D. Lee, R. Studart, B. Wang, C.-H. Chen, J. Thiele, R. K. Shah, A. Krummel and D. A. Weitz, *Macromolecular Rapid Communication*, 2010, **31**, 108-118.

17. J. Guzowski, P. M. Korczyk, S. Jakiela and P. Garstecki, *Soft Matter*, 2012, **8**, 7269-7278.
18. N. Pannacci, H. Bruus, D. Bartolo, I. Etchart, T. Lockhart, Y. Hennequin, H. Willaime and P. Tabeling, *Physical Review Letters*, 2008, **101**, 16450.
19. H. Hasinovic and S. E. Friberg, *Journal of Colloid and Interface Science*, 2011, **361**, 581-586.
- 5 20. H. Hasinovic and S. E. Friberg, *Langmuir*, 2011, **27**, 6584-6588.
21. H. Hasinovic, S. E. Friberg and G. Rong, *Journal of Colloid and Interface Science*, 2011, **354**, 424-426.
22. H. Hasinovic, C. Boggs, S. E. Friberg, I. Kovach and J. Koetz, *Journal of Dispersion Science and Technology*, 2013, DOI: 10.1080/01932691.2013.801019.
- 10 23. N. Rashnidia and R. Balusbraminian, *D Del Signore AIChE J* 1992, 665.
24. A. El-Hamouz, *Journal of Dispersion Science and Technology*, 2007, **28**, 797-804.
25. A. Atist, S. SBagwat, K. W. Penfield and P. A. Aikens, *J surfactants Detergents*, 2000, **3**, 53.
26. G. Kaptay, *Metallurgical and Materials Transactions B*, 2001, **32B**, 555-557.
27. S. E. Friberg, I. Kovach and J. Koetz, *ChemPhysChem*, 2013, **14**, 3772-3776.
- 15 28. S. E. Friberg, *Journal of Colloid and Interface Science*, 2014, **416**, 167-171.
29. K. W. Desmond, P. J. Young, D. Chen and E. R. Weeks, *Soft Matter*, 2013, **9**, 3424-3436.
30. P. DeGennes, *Rev Mod Phys*, 1985, **57**, 827-863.
31. A. Amirfazli and A. W. Neumann, *Advances in Colloid and Interface Science*, 2004, **110**, 121-141.
32. D. Exerowa and D. Platikanov, *Advances in Colloid and Interface Science*, 2009, **147-148**, 74-87.
- 20 33. H. Hasinovic, S. E. Friberg, I. Kovach and J. Koetz, *Journal of Dispersion Science and Technology*, 2013, **34**, 1683-1689.

Figures:

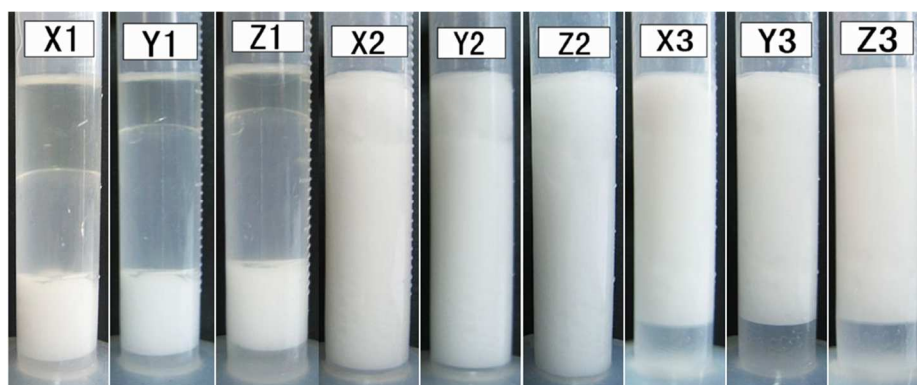


Figure 1. Digital photographs of emulsions in series 1, 2, and 3 with initial compositions shown in Table 1.

The volume ratio of VO/SO in each series decreases from left to right. The photograph is taken at 24 h

after the emulsification when the development of each layer reaches a stable state.

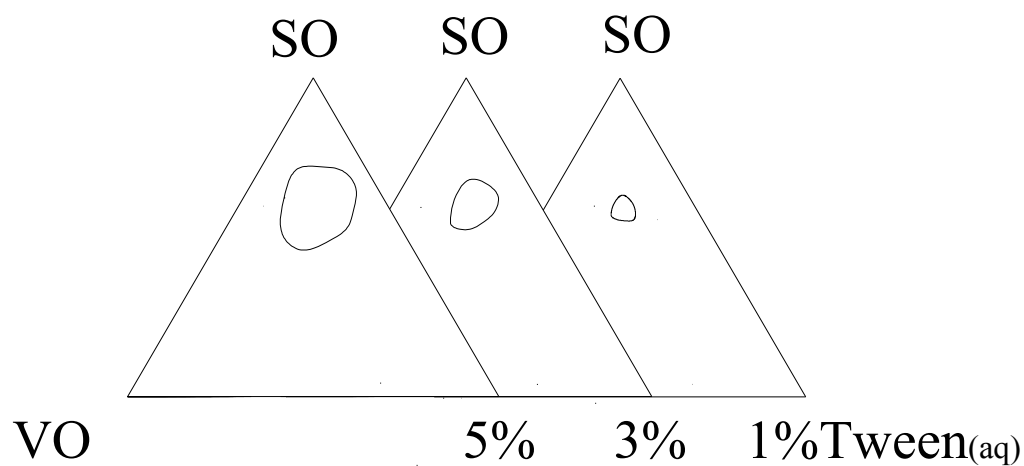


Figure 2. The composition areas for stable Janus emulsions.

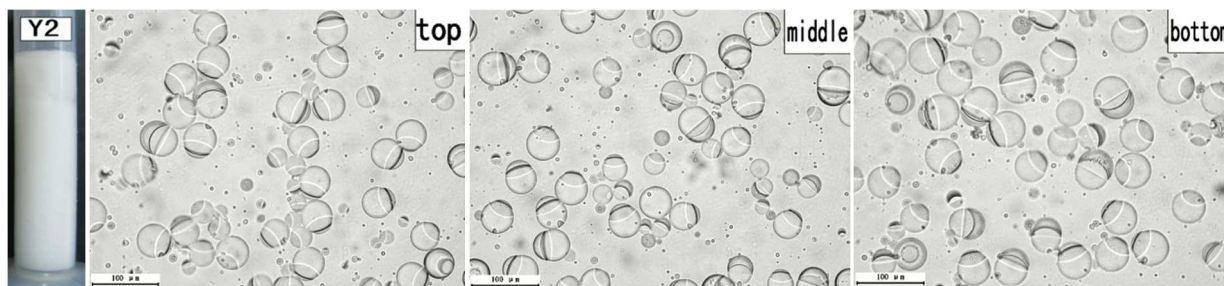


Figure 3. Optical microscopy images in different heights of emulsion Y2. The composition of emulsion Y2 is shown in Table 2. All the scale bars are 100 μm .

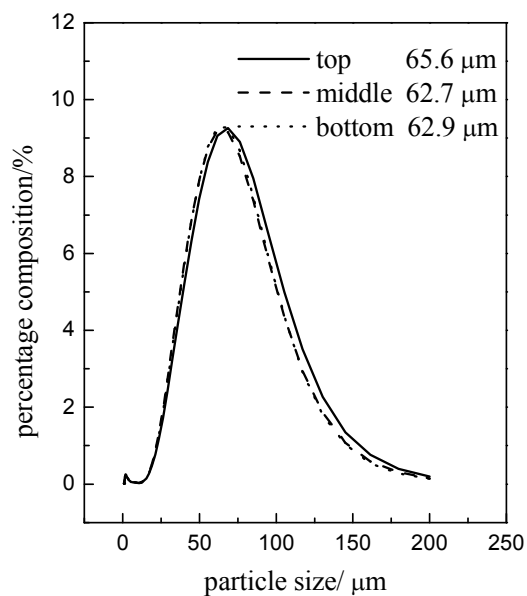


Figure 4. Size distributions of emulsion droplets in different heights of emulsion Y2. Composition of emulsions Y2 is shown in Table 2. The numbers in the graph show the mean average diameters of Janus emulsion droplets.

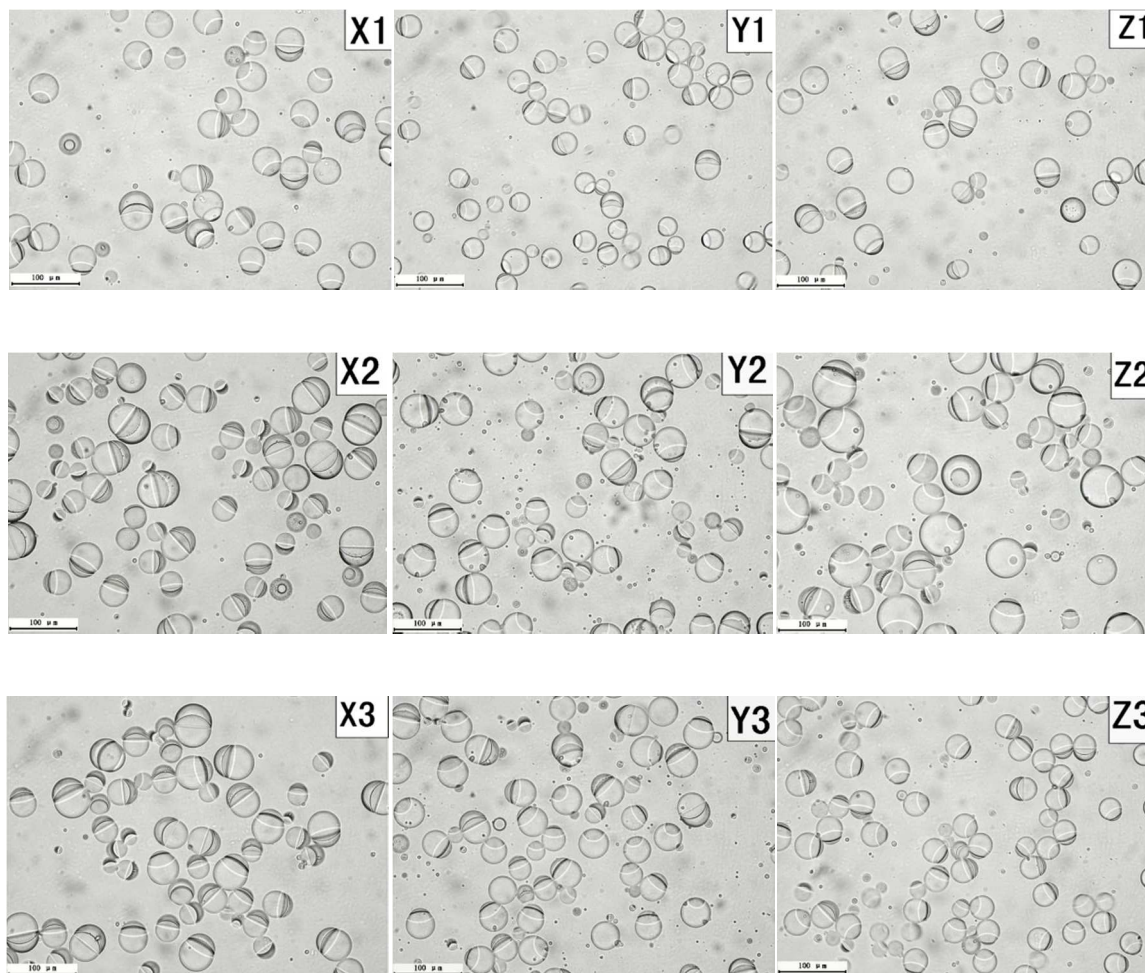


Figure 5. Optical microscopy images of emulsions with final compositions shown in Table 2. All the scale bars are 100 μm .

5

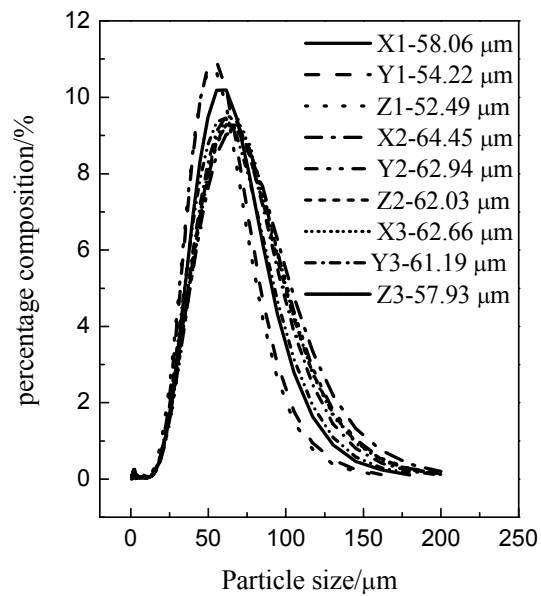


Figure 6. Size distributions of stable emulsions with final compositions shown in Table 2. The numbers in the graph show the mean average diameter of Janus emulsion droplets.

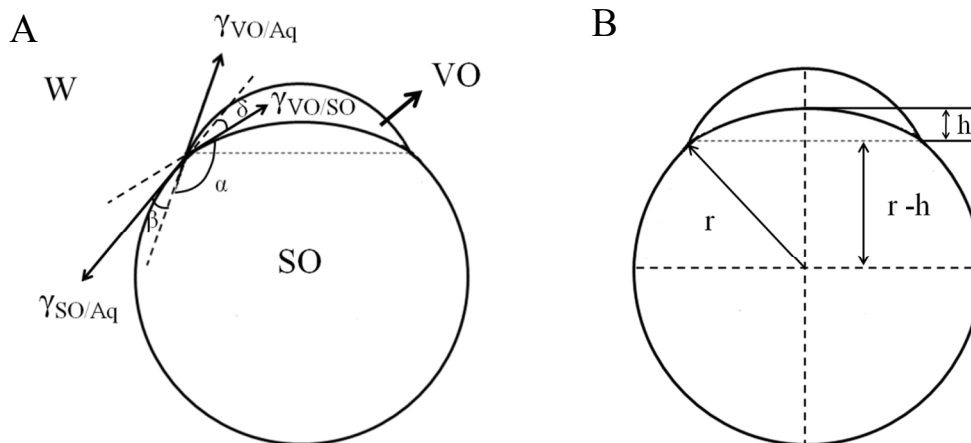


Figure 7. Illustrations of the cross-section of the Janus droplet.

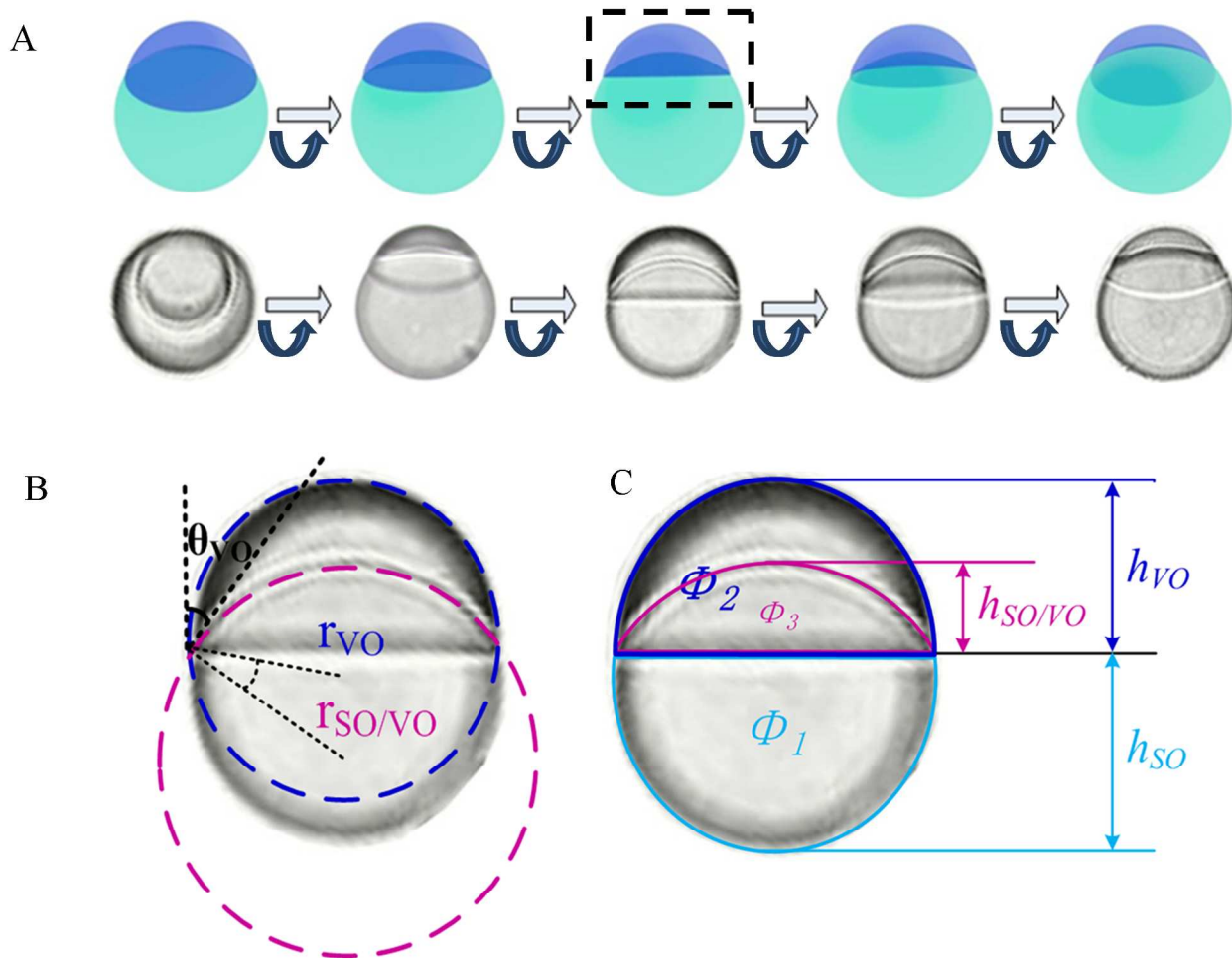


Figure 8. A-Five typical projections of Janus droplets in bulk. Image in the frame corresponds to the case with the plane of contact circle parallel to the sight line; B-Illustration of contact angle of VO caps; C-Illustration of the volume and the heights of three caps.

Tables:

TABLE 1: Volumes (/mL) of the Samples in the System of SO/VO/Aq with Weight Fractions of Aq in Three Series 0.10, 0.20, 0.30. Concentration of Tween 80 in Aq is 3.0 wt%.

| Series 1 | Aq=0.10 | | | Series 2 | Aq=0.20 | | | Series 3 | Aq=0.30 | | |
|----------|---------|------|------|----------|---------|------|------|----------|---------|------|------|
| | VO | SO | Aq | | VO | SO | Aq | | VO | SO | Aq |
| X1 | 1.96 | 3.72 | 0.59 | X2 | 1.79 | 3.30 | 1.24 | X3 | 1.50 | 2.93 | 1.79 |
| Y1 | 1.19 | 4.51 | 0.59 | Y2 | 1.05 | 3.97 | 1.21 | Y3 | 0.95 | 3.48 | 1.82 |
| Z1 | 0.87 | 4.80 | 0.60 | Z2 | 0.71 | 4.29 | 1.19 | Z3 | 0.67 | 3.72 | 1.80 |

TABLE 2: Composition of Stable Emulsion (Em) Layer and Average Topology Parameters of Individual Janus Droplets Obtained from Microscopy Image.

| | Composition in Em layer | | Parameters of individual Janus Droplets | | |
|----|-------------------------|------|-----------------------------------------|----------------------|-------------|
| | VO/SO | Aq | VO/SO | $\theta_{VO}/^\circ$ | τ_{cp} |
| X1 | 0.11 | 0.25 | 0.11±0.04 | 34 | 0.422 |
| Y1 | 0.16 | 0.29 | 0.13±0.05 | 35 | 0.447 |
| Z1 | 0.12 | 0.24 | 0.15±0.08 | 35 | 0.441 |
| X2 | 0.54 | 0.19 | 0.48±0.16 | 37 | 0.470 |
| Y2 | 0.26 | 0.18 | 0.28±0.14 | 38 | 0.466 |
| Z2 | 0.17 | 0.19 | 0.14±0.07 | 35 | 0.442 |
| X3 | 0.51 | 0.19 | 0.50±0.18 | 38 | 0.478 |
| Y3 | 0.27 | 0.20 | 0.27±0.11 | 36 | 0.449 |
| Z3 | 0.18 | 0.20 | 0.12±0.05 | 36 | 0.441 |

Note: The error of θ_{VO} is within $\pm 2.3^\circ$

TABLE 3: Parameters of Individual Janus Droplets Calculated from Interfacial Tension (mN/m) by Assuming Local Equilibrium, and Average Results Obtained from Microscopy Images. The Emulsion Composition is VO/SO=0.25, and Weight Fraction of Aq=0.20.

| wt% Tween 80 in Aq | Calculated results from interfacial tension | | | | | | Parameters from microscopy image | | |
|-----------------------|---------------------------------------------|------------------|----------|---------|----------|-----------------------|----------------------------------|-------------|-----------|
| | $\gamma_{VO/Aq}$ | $\gamma_{SO/Aq}$ | α | β | δ | θ_{VO}° | θ_{VO}° | τ_{CP} | VO/SO |
| 0.1 | 8.18 | 10.51 | 153 | 6 | 22 | 27 | 30 | 0.462 | 0.26±0.10 |
| 0.5 | 7.72 | 9.96 | 148 | 8 | 25 | 32 | 33 | 0.456 | 0.27±0.13 |
| 1 | 7.46 | 9.67 | 146 | 9 | 26 | 34 | 33 | 0.457 | 0.23±0.11 |
| 3 | 7.22 | 9.39 | 144 | 9 | 27 | 36 | 36 | 0.466 | 0.28±0.12 |
| 5 | 7.12 | 9.20 | 140 | 10 | 30 | 40 | 37 | 0.454 | 0.25±0.14 |
| 9 | 7.14 | 9.23 | 140 | 10 | 30 | 40 | 39 | 0.457 | 0.26±0.12 |

Notes: 1 Definitions of α , β , δ are illustrated in Figure 7, and the location of contact plane τ_{CP} is explained in equation (6); 2 Interfacial tension between VO and SO is 2.54 mN/m. The angle θ_{VO} of VO caps equals to $\beta+\delta$; 3 Error of θ_{VO} value obtained from microscope images is $\pm 2.3^{\circ}$.

TABLE 4: Essential Topology and Free Energy Parameters for the Separated and Janus Droplets

| Compound | Radius/m | | Volume/m ³ | Interface area/ m ² | | Surface free energy/J | |
|-----------|----------|-------|-----------------------|--------------------------------|----------|-----------------------|----------|
| | Separate | Janus | - | Separate | Janus | Separate | Janus |
| VO | 17.7E-6 | 30E-6 | 1.77E-14 | 3.28E-9 | 2.83E-09 | 2.37E-11 | 2.04E-11 |
| SO | 28.3E-6 | 30E-6 | 9.54E-14 | 1.01E -8 | 8.48E-09 | 9.48E-11 | 7.96E-11 |
| interface | - | 35E-6 | - | - | 3.30E-09 | - | 8.38E-12 |
| total | - | - | 1.13E-13 | 1.34E-8 | 1.46E-08 | 1.19E-10 | 1.08E-10 |

Note: $h = r/2 = 30E-6m$. $\gamma_{VO/Aq} = 7.22$ mN, $\gamma_{SO/Aq} = 9.39$ mN, $\gamma_{VO/SO} = 2.54$ mN.

Supporting Information:

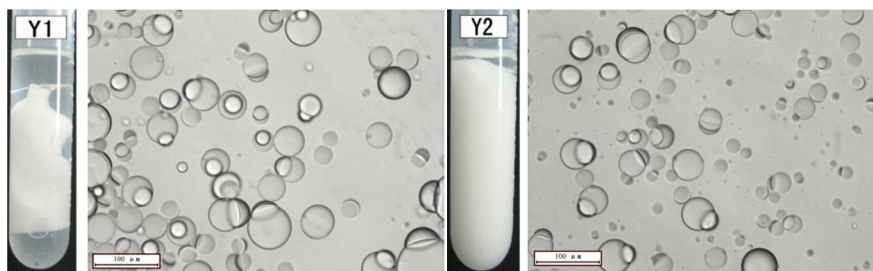


Figure S1. Optical microscopy images of emulsions Y1 and Y2 six months after preparation. The compositions of emulsions are shown in Table 1. The top layer of Y2 is VO phase.

5

TABLE S1: Volumes (/mL) of Each Layer Separated of Samples in Figure 1 after 24h.

| | Series 1 | | | | Series 2 | | | | Series3 | | | | | |
|----|----------|------|------|------|----------|----|----|------|---------|----|----|----|------|------|
| | VO | SO | Em | Aq | VO | SO | Em | Aq | VO | SO | Em | Aq | | |
| X1 | 1.82 | 2.42 | 1.82 | 0.14 | X2 | - | - | 6.02 | 0.14 | X3 | - | - | 5.38 | 0.78 |
| Y1 | 1.03 | 3.49 | 1.61 | 0.12 | Y2 | - | - | 6.14 | 0.13 | Y3 | - | - | 5.37 | 0.78 |
| Z1 | 0.74 | 3.68 | 1.59 | 0.23 | Z2 | - | - | 6.11 | 0.10 | Z3 | - | - | 5.52 | 0.72 |

TABLE S2: Maximum and Minimum Values of Weight Fractions of Aq and VO/SO Weight Ratios in the “Stable Janus emulsion” Region of the Partial Phase Map in Figure 2

| wt% Tween 80 in Aq | Aq | | VO/SO | |
|-----------------------|---------|---------|---------|---------|
| | Maximum | Minimum | Maximum | Minimum |
| 1 | 0.26 | 0.18 | 0.41 | 0.27 |
| 3 | 0.29 | 0.16 | 0.55 | 0.15 |
| 5 | 0.33 | 0.10 | 0.69 | 0.06 |

5

